Peristaltic Transport of a Viscoelastic Fluid with Fractional Maxwell Model in an Inclined Channel

Ali Ibrahim .A.H. *, Ahmed M. Abdulhadi
Department of Mathematics, College of Science, University of Baghdad, Baghdad, Iraq.

Abstract

This paper is devoted to the study of the peristaltic transport of viscoelastic non-Newtonian fluids with fractional Maxwell model in an inclined channel. Approximate analytical solutions have been constructed using Adomain decomposition method under the assumption of long wave boundary layer type approximation and low Reynolds number. The effect of each of relaxation time, fractional parameters, Reynolds number, Froude number, inclination of channel and amplitude on the pressure difference, friction force and stream function along one wavelength are received and analyzed.

Keywords: Peristaltic transport, Fractional Maxwell model, Pressure difference, Friction force, Adomian decomposition method

الانتقال التموجي لسائل لزج لا نيوتوني لنموذج ماكسويل الكسري في قناة مائلة

علي ابراهيم عبد الحسين*، احمد مولود عبد الهادي
قسم الرياضيات، كلية العلوم، جامعة بغداد، بغداد، العراق.

الخلاصة

في هذا البحث درسنا الانتقال التموجي لسائل لزج لا نيوتوني لنموذج ماكسويل الكسري في قناة مائلة. تم الحصول على الحلول التحليلية التقريبة بأستخدام طريقة (Adomain) للتجزئة تحت فرضية الطبقة الحدودية الموجية طويلة وفرضية ان يكون عدد رينولد صغير. تأثير كلا من زمن التمدد، المعلمات الكسرية، عدد رينولدز، عدد فرويد، زاوية ميل القناة وكذالك سعتها على اختلاف الضغط ، قوة الاحتكاك و دالة التدفق خلال طول موجي واحد قد تم ايجادها و تحليلها

1. Introduction

Peristalsis is an important mechanism for mixing and transporting fluids, which is generated by a progressive wave of contraction or expansion moving on the wall of the tube. Physiological fluids in animal and human bodies are, in general, pumped by the continuous periodic muscular oscillations of the ducts. These oscillations are presumed to be caused by the progressive transverse contraction waves that propagate along the walls of the ducts. Peristalsis is the mechanism of the fluid transport that occurs generally from a region of lower pressure to higher pressure when a progressive wave of area contraction and expansion travels along the flexible wall of the tube. Peristaltic flows occurs widely in the functioning

*Email:Ali_ibrahim741990@yahoo.com

of the ureter, food mixing and chime movement in the intestine, movement of eggs in the fallopian tube, the transport of the spermatozoa in cervical canal, transport of bile in the bile duct, transport of cilia, and circulation of blood in small blood vessels[1].

The study of peristaltic motion in both mechanical and physiological situations has been studied in Refs. [2–5]. Shapiro et al. [5] have investigated the peristaltic pumping under assumptions of long wavelength and low Reynolds number. They have considered two-dimensional and axisymmetric flows of Newtonian fluids and they discussed the mechanical efficiency and some important phenomena of peristaltic pump such as reflux and trapping. Their investigation is focused only about Newtonian fluids and does not over the peristaltic flow of other fluids such as non-Newtonian fluids.

The non-Newtonian fluids are being considered more important and appropriate in view of engineering and biological applications as compared with the Newtonian fluids. Viscoelastic fluid is a non-Newtonian fluid, which contains both viscous and elastic properties. Most of the biological fluids such as blood, chyme, and food bolus are found to be viscoelastic in nature. Bohme and Friedrich [6] studied peristaltic flow of viscoelastic liquids. Some other workers [7–11] have investigated peristaltic transport of viscoelastic fluid with Maxwell model and they have discussed the effect of relaxation time on the peristaltic transport. Hayat et al. [12–15] have investigated the peristaltic transport of viscoelastic fluids with Jeffrey model and they have also discussed the effect of relaxation and retardation time on the peristaltic transport.

The constitutive equations with ordinary and fractional time derivatives have been introduced to describe the viscoelastic properties of materials in various fields. Rheological models with fractional time derivatives have played an important role in the study of the valuable tool of viscoelastic properties. In general, fractional Maxwell model is derived from the well known Maxwell model by replacing ordinary derivatives of shear stress-strain relationship by derivatives of fractional order.

Recently, Tripathi et al. [16] have incorporated the application of fractional element models of viscoelastic materials in the study of bio-fluids flow. They discussed the effects of fractional parameters and relaxation time on peristaltic flow. This result has been again extended for generalized fractional Maxwell model, fractional second grade model and fractional Oldroyd-B model [17–19].

In this paper we consider the peristaltic transport of viscoelastic non-Newtonian fluids with fractional Maxwell model in an inclined channel under the assumption of long wavelength and low Reynolds number. We have discussed the effects of relaxation time, fractional parameters, Reynolds number, Froude number, inclination of channel and amplitude on the pressure difference and friction force along one wavelength. Adomain decomposition method used to obtain the analytical approximate solutions of the fractional differential equation.

2. Mathematical model

When the wall of the channel is brought under the influence of a periodic radial contraction wave, a part of the wall begins to contract initially at the inlet, which then relaxes and the portion lying ahead of this begins to contract showing that the contraction wave progresses towards the outlet. Relaxation culminates at the natural boundary without expanding further beyond it. This process continues until complete transportation takes place. Such a motion figure-1 may be mathematically modeled as [20]

$$\tilde{h}(\tilde{\xi},\tilde{t}) = a - \frac{1}{2}\tilde{\phi}\left(1+\cos\frac{2\pi}{\lambda}(\tilde{\xi}-c\tilde{t})\right) \tag{1}$$

where $\tilde{\xi},\tilde{t}$, a, $\tilde{\phi}$, λ, c, $\tilde{h}$ are respectively axial coordinate, time, the semi-width of the channel, amplitude of wave, wavelength, wave velocity and transverse displacement of the walls from the center line.

The constitutive equation of shear stress-strain relationship of viscoelastic fluid with fractional Maxwell model is given by

$$\left(1+\tilde{\lambda}_1^{\alpha}\frac{\partial^{\alpha}}{\partial\tilde{t}^{\alpha}}\right)\tilde{\tau}=G\tilde{\lambda}_1^{\beta}\frac{\partial^{\beta}\gamma}{\partial\tilde{t}^{\beta}}, \tag{2}$$

where, $\tilde{\lambda}_1,\tilde{\tau},\gamma$ are the relaxation time, shear stress, shear strain, $G=\mu/\tilde{\lambda}_1$ is the shear modulus, μ is the viscosity and $\alpha,\ \beta$ are the fractional parameters such that $0\le\alpha\le\beta\le 1$. This model reduces to ordinary Maxwell model if $\alpha=\beta=1$ and Classical Navier Stokes model, when $\alpha=0,\ \beta=0$.

The governing equations of motion for incompressible fluids in two-dimensional case for inclined channel flow are given by

$$\left.\begin{aligned}\rho\left(\frac{\partial}{\partial\tilde{t}}+\tilde{u}\frac{\partial}{\partial\tilde{\xi}}+\tilde{v}\frac{\partial}{\partial\tilde{\eta}}\right)\tilde{u}&=-\frac{\partial\tilde{p}}{\partial\tilde{\xi}}+\rho g\sin A+\frac{\partial\tilde{\tau}_{\tilde{\xi}\tilde{\xi}}}{\partial\tilde{\xi}}+\frac{\partial\tilde{\tau}_{\tilde{\xi}\tilde{\eta}}}{\partial\tilde{\eta}},\\ \rho\left(\frac{\partial}{\partial\tilde{t}}+\tilde{u}\frac{\partial}{\partial\tilde{\xi}}+\tilde{v}\frac{\partial}{\partial\tilde{\eta}}\right)\tilde{v}&=-\frac{\partial\tilde{p}}{\partial\tilde{\eta}}-\rho g\cos A+\frac{\partial\tilde{\tau}_{\tilde{\eta}\tilde{\xi}}}{\partial\tilde{\xi}}+\frac{\partial\tilde{\tau}_{\tilde{\eta}\tilde{\eta}}}{\partial\tilde{\eta}}\end{aligned}\right\} \tag{3}$$

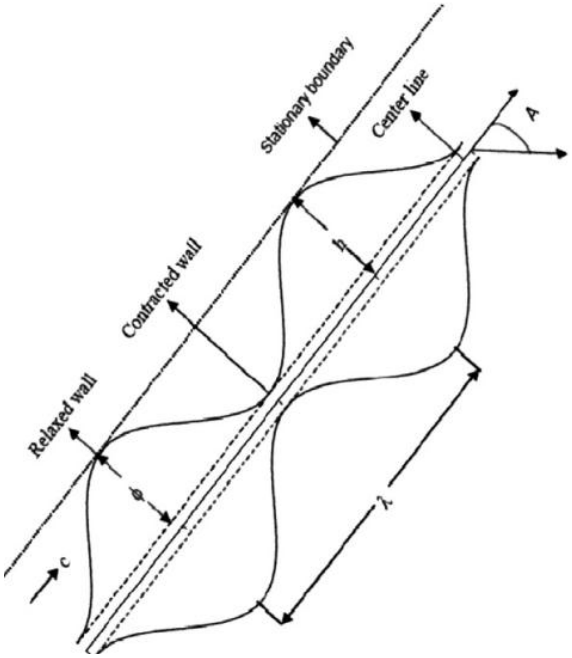

Figure 1- Geometry of wall surface with inclination of angle A.

where, $\rho,\tilde{u}\ ,\tilde{v},\tilde{\eta},\tilde{p},g,A,$ are the fluid density, velocity, transverse velocity, transverse coordinate, pressure, acceleration due to the gravity and inclination angle of channel, respectively.

The physical parameters are non-dimensionalized as follows:

$$\left.\begin{aligned} &\xi=\frac{\tilde{\xi}}{\lambda},\ \eta=\frac{\tilde{\eta}}{a},\ \lambda_1=\frac{c\tilde{\lambda}_1}{\lambda},t=\frac{c\tilde{t}}{\lambda},u=\frac{\tilde{u}}{c},v=\frac{\tilde{v}}{c\delta},h=\frac{\tilde{h}}{a},\\ &\phi=\frac{\tilde{\phi}}{a},\delta=\frac{a}{\lambda},p=\frac{\tilde{p}a^2}{\mu c\lambda},\tau=\frac{a\tilde{\tau}}{\mu c},\mathrm{Re}=\frac{\rho ca\delta}{\mu},Fr=\frac{c^2}{ga}\end{aligned}\right\} \tag{4}$$

where Re, Fr and δ stand for the Reynolds number, Froude number and wave number respectively. We introduce the non-dimensional parameters, Eq.(1) reduces to

$$h(\xi,t)=1-\phi\cos^2\pi(\xi-t), \tag{5}$$

and under the assumptions of long wavelength and low Reynolds number, Eq. (3) reduce to

$$\left.\begin{aligned} &\left(1+\lambda_1^{\alpha}\frac{\partial^{\alpha}}{\partial t^{\alpha}}\right)\left(\frac{\partial p}{\partial\xi}-\frac{\mathrm{Re}}{Fr}\sin A\right)=\lambda_1^{\beta-1}\frac{\partial^{\beta-1}}{\partial t^{\beta-1}}\left(\frac{\partial^2 u}{\partial\eta^2}\right),\\ &\frac{\partial p}{\partial\eta}=0.\end{aligned}\right\} \tag{6}$$

Boundary conditions are given by

$$\frac{\partial(\xi,t)}{\partial\eta}=0\ at\ \eta=0 \tag{7}$$

$$u(\xi,t)=0\ at\ \eta=h \tag{8}$$

$$\frac{\partial p}{\partial\xi}=0\ at\ t=0 \tag{9}$$

Integrating Eq. (6) with respect to η, and using (7) we get

$$\left(1+\lambda_1^{\alpha}\frac{\partial^{\alpha}}{\partial t^{\alpha}}\right)\left(\frac{\partial p}{\partial\xi}-\frac{\mathrm{Re}}{Fr}\sin A\right)\eta=\lambda_1^{\beta-1}\frac{\partial^{\beta-1}}{\partial t^{\beta-1}}\left(\frac{\partial u}{\partial\eta}\right) \tag{10}$$

Further integrating Eq. (10) from h to η, yields

$$\frac{\partial^{\beta-1}u}{\partial t^{\beta-1}}=\frac{\lambda_1^{-(\beta-1)}}{2}\left(1+\lambda_1^{\alpha}\frac{\partial^{\alpha}}{\partial t^{\alpha}}\right)\left(\frac{\partial p}{\partial\xi}-\frac{\mathrm{Re}}{Fr}\sin A\right)(\eta^2-h^2) \tag{11}$$

The volume flow rate is defined as $Q=\int_0^h u\,d\eta,$ which, by virtue of Eq.(11), reduces to

$$\frac{\partial^{\beta-1}\mathrm{Q}}{\partial t^{\beta-1}},=\frac{-h^3\lambda_1^{-(\beta-1)}}{3}\left(1+\lambda_1^{\alpha}\frac{\partial^{\alpha}}{\partial t^{\alpha}}\right)\left(\frac{\partial p}{\partial \xi}-\frac{\mathrm{Re}}{Fr}\sin A\right) \tag{12}$$

The transformations between the wave and the laboratory frames, in the dimensionless form, are given by

$$x=\xi-t,\ y=\eta, U=u-1,\ q=\mathrm{Q}-h \tag{13}$$

where, the left side parameters are in the wave frame and the right side parameters are in the laboratory frame.

The averaged flow rate $\overline{\mathrm{Q}}$ is given by

$$\overline{\mathrm{Q}}=\int_0^1 \mathrm{Q}\,\mathrm{dt}=\int_0^1 (q+h)dt=q+1-\frac{\phi}{2} \tag{14}$$

Eq.(12), in view of Eqs.(13) and (14) gives

$$-3\lambda_1^{\beta-\alpha-1}\frac{\partial^{\beta-1}}{\partial t^{\beta-1}}\left(\frac{\overline{\mathrm{Q}}\text{-}1+\mathrm{h}+\frac{\phi}{2}}{h^3}\right)=\frac{1}{\lambda_1^{\alpha}}\left(\frac{\partial p}{\partial x}-\frac{\mathrm{Re}}{Fr}\sin A\right)+\frac{\partial^{\alpha}}{\partial t^{\alpha}}\left(\frac{\partial p}{\partial x}-\frac{\mathrm{Re}}{Fr}\sin A\right) \tag{15}$$

In the last equation, if we set A= 0, we obtain the corresponding equation for viscoelastic non-Newtonian fluid (horizontal channel) as obtained by Tripathi [16,Eq.(12)].

From Eq. (11), and using Eqs. (12) and (14), the stream function (ψ) in wave frame $(U=\frac{\partial \psi}{\partial y})$ is obtained as

$$\psi=-\left(y^3-3yh^2\right)\left(\frac{\overline{\mathrm{Q}}+h-1+\frac{\phi}{2}}{2h^3}\right)-y \tag{16}$$

It is clear from Eq. (16) that the stream function is independent of fractional parameters, material constants, Reynolds number, Froude number and inclination angle of channel.

3. Solution of the problem

Eq.(15) can be rewritten as

$$-\lambda_1^{\beta-\alpha-1}\frac{\partial^{\beta-1}\lambda_2}{\partial t^{\beta-1}}=\frac{1}{\lambda_1^{\alpha}}f+\frac{\partial^{\alpha}}{\partial t^{\alpha}}f \tag{17}$$

where, $f(x,t)=\frac{\partial p}{\partial x}-\frac{\mathrm{Re}}{Fr}\sin A,$ and $\lambda_2=3\left(\frac{\overline{\mathrm{Q}}\text{-}1+\mathrm{h}+\frac{\phi}{2}}{h^3}\right).$

with the initial condition

$$f(x,0)=-\frac{\mathrm{Re}}{Fr}\sin A \tag{18}$$

We consider the Eq. (17) as

$$\frac{\partial f}{\partial t}=-\frac{\partial^{1-\alpha}}{\partial t^{1-\alpha}}\left[\frac{1}{\lambda_1^{\alpha}}f+\frac{\lambda_1^{\beta-\alpha-1}\lambda_2}{\Gamma(2-\beta)}t^{1-\beta}\right],$$

$$L_t f=-\frac{\partial^{1-\alpha}}{\partial t^{1-\alpha}}\left[\frac{1}{\lambda_1^{\alpha}}f+\frac{\lambda_1^{\beta-\alpha-1}\lambda_2}{\Gamma(2-\beta)}t^{1-\beta}\right] \tag{19}$$

where $L_t\equiv\partial/\partial t$ symbolizes the linear differential operation.

Applying the integration inverse operator $L_t^{-1}=\int_0^t(\bullet)dt$, to the Eq. (19) and using Eq. (18), we get

$$f(x,t)=-L_t^{-1}\frac{\partial^{1-\alpha}}{\partial t^{1-\alpha}}\left[\frac{1}{\lambda_1^{\alpha}}f+\frac{\lambda_1^{\beta-\alpha-1}\lambda_2}{\Gamma(2-\beta)}t^{1-\beta}\right]-\frac{\mathrm{Re}}{Fr}\sin A \tag{20}$$

The ADM assumes infinite series solutions for unknown function $f(x,t)$ and it is given by

$$f(x,t)=\sum_{n=0}^{\infty}f_n(x,t) \tag{21}$$

where, the components $f_0,\ f_1,\ f_2,...,\ f_{n+1}$ are usually determined recursively by

$$f_0=-\frac{\mathrm{Re}}{Fr}\sin A,$$

$$f_1=-L_t^{-1}\frac{\partial^{1-\alpha}}{\partial t^{1-\alpha}}\left[\frac{1}{\lambda_1^{\alpha}}f_0+\frac{\lambda_1^{\beta-\alpha-1}\lambda_2}{\Gamma(2-\beta)}t^{1-\beta}\right]$$

$$f_2 = -L_t^{-1}\frac{\partial^{1-\alpha}}{\partial t^{1-\alpha}}\left[\frac{1}{\lambda_1^{\alpha}}\, f_1 + \frac{\lambda_1^{\beta-\alpha-1}\lambda_2}{\Gamma(2-\beta)}t^{1-\beta}\right]$$

$$f_{n+1} = -L_t^{-1}\frac{\partial^{1-\alpha}}{\partial t^{1-\alpha}}\left[\frac{1}{\lambda_1^{\alpha}}\, f_n + \frac{\lambda_1^{\beta-\alpha-1}\lambda_2}{\Gamma(2-\beta)}t^{1-\beta}\right], \qquad n \geq 0 \qquad (22)$$

and the values are obtained as

$$f_0 = -\frac{\mathrm{Re}}{Fr}\sin A,$$

$$f_1 = \frac{\mathrm{Re}\; t^{\alpha}\sin A}{Fr\,\lambda_1^{\alpha}\,\Gamma(\alpha+1)} - \frac{\lambda_2\, t^{\alpha-\beta+1}}{\lambda_1^{\alpha-\beta+1`}\,\Gamma(\alpha-\beta+2)},$$

$$f_2 = -\frac{\mathrm{Re}\; t^{2\alpha}\sin A}{Fr\,\lambda_1^{2\alpha}\,\Gamma(2\alpha+1)} + \lambda_2\left[\frac{t^{2\alpha-\beta+1}}{\lambda_1^{2\alpha-\beta+1`}\,\Gamma(2\alpha-\beta+2)} - \frac{t^{\alpha-\beta+1}}{\lambda_1^{\alpha-\beta+1`}\,\Gamma(\alpha-\beta+2)}\right],$$

$$f_3 = \frac{\mathrm{Re}\; t^{3\alpha}\sin A}{Fr\,\lambda_1^{3\alpha}\,\Gamma(3\alpha+1)} + \lambda_2\left[\begin{array}{l}\dfrac{-t^{3\alpha-\beta+1}}{\lambda_1^{3\alpha-\beta+1`}\,\Gamma(3\alpha-\beta+2)} + \dfrac{t^{2\alpha-\beta+1}}{\lambda_1^{2\alpha-\beta+1`}\,\Gamma(2\alpha-\beta+2)} - \\ \dfrac{t^{\alpha-\beta+1}}{\lambda_1^{\alpha-\beta+1`}\,\Gamma(\alpha-\beta+2)}\end{array}\right],$$

$$f_4 = \frac{\mathrm{Re}\; t^{4\alpha}\sin A}{Fr\,\lambda_1^{4\alpha}\,\Gamma(4\alpha+1)} + \lambda_2\left[\begin{array}{l}\dfrac{t^{4\alpha-\beta+1}}{\lambda_1^{4\alpha-\beta+1`}\,\Gamma(4\alpha-\beta+2)} - \dfrac{t^{3\alpha-\beta+1}}{\lambda_1^{3\alpha-\beta+1`}\,\Gamma(3\alpha-\beta+2)} + \\ \dfrac{t^{2\alpha-\beta+1}}{\lambda_1^{2\alpha-\beta+1`}\,\Gamma(2\alpha-\beta+2)} - \dfrac{t^{\alpha-\beta+1}}{\lambda_1^{\alpha-\beta+1`}\,\Gamma(\alpha-\beta+2)}\end{array}\right],$$

$$f_{n+1} = \frac{\mathrm{Re}\; t^{(n+1)\alpha}\sin A}{Fr\,\lambda_1^{(n+1)\alpha}\,\Gamma((n+1)\alpha+1)} + \lambda_2\left[\begin{array}{l}\dfrac{t^{(n+1)\alpha-\beta+1}}{\lambda_1^{(n+1)\alpha-\beta+1`}\,\Gamma((n+1)\alpha-\beta+2)} - \dfrac{t^{n\alpha-\beta+1}}{\lambda_1^{n\alpha-\beta+1`}\,\Gamma(n\alpha-\beta+2)} + \\ \cdots - \dfrac{t^{\alpha-\beta+1}}{\lambda_1^{\alpha-\beta+1`}\,\Gamma(\alpha-\beta+2)}\end{array}\right],$$

Proceeding in similar manner, the components $f_n(x,t),\ n \geq 0$ are obtained and finally the series solutions are thus entirely determined. Again, if we set A= 0, we obtain the corresponding equation for viscoelastic non-Newtonian fluid (horizontal channel) as obtained by Tripathi [16,Eq.(19)]. Finally, we approximate the solution $f(x,t)$, by the truncating the series

$$f(x,t) = \frac{\partial p}{\partial x} - \frac{\mathrm{Re}}{Fr}\sin A = \lim_{N\to\infty} \Phi_N(x,t) \tag{23}$$

where, $\Phi_N(x,t) = \sum_{n=0}^{N-1} f_n(x,t)$. From Eq. (23), the pressure gradient is given as

$$\frac{\partial p}{\partial x} = \frac{\mathrm{Re}}{Fr}\sin A + \lim_{N\to\infty} \Phi_N(x,t),$$

The pressure difference (Δp) and friction force (F) across one wavelength are given by

$$\Delta p = \int_0^1 \frac{\partial p}{\partial x}\, dx \tag{24}$$

$$F = \int_0^1 -h\frac{\partial p}{\partial x}\, dx \tag{25}$$

4. Numerical results and discussion

In this section numerical results are displayed through figure-2 to figure–16 to show the effects of various parameters such as fractional parameters (α,β), relaxation time (λ_1), time (t), amplitude (ϕ), Reynolds number (Re), Froude number (Fr), the inclination angle (A) on the pressure difference and friction force across one wavelength. In order to estimate the quantitative effects of the various parameters involved in the results of the present analysis, we used the MATHEMATICA software. It is noted that only ten terms of the series are used in evaluating the approximate solutions. It is evident that the solution can be improved by further computing more terms.

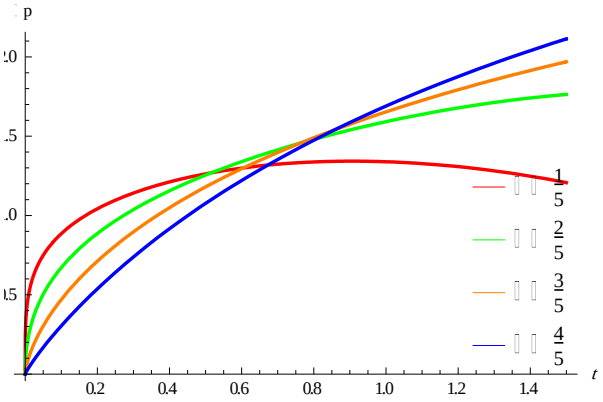

Figure 2-Pressure vs. time at $\overline{Q}$ =0.1, $\phi = 0.5, \beta = 4/5$, $\lambda_1 = 1,\ \mathrm{Re} = 0.01,\ Fr = 0.01,\ A = \pi/3$

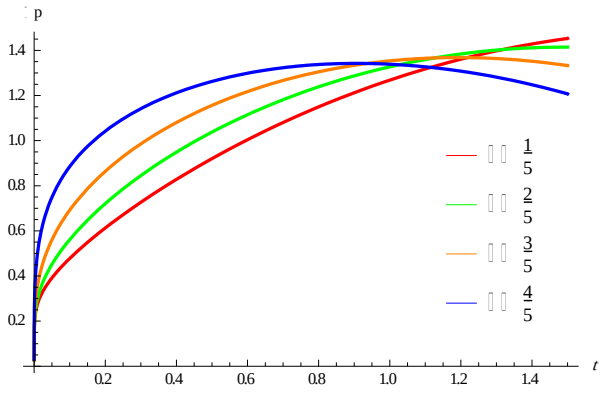

Figure 3- Pressure vs. time at $\overline{Q}$ =0.1, $\phi = 0.5$, $\lambda_1 = 1,\ \mathrm{Re} = 0.01,\ Fr = 0.01,\ A = \pi/3,\ \alpha = 1/5$.

In figure-2, the variation of Δp vs. time t, is shown for different values of α =1/5, 2/5, 3/5, 4/5 by fixing other parameters $\overline{Q}$ =0.1, $\phi = 0.5, \beta = 4/5$, $\lambda_1 = 1$, $\mathrm{Re} = 0.01$, $Fr = 0.01$, $A = \pi/3$. As expected, there is a nonlinear relation between pressure and time. It is worth mentioning that increase in time raises pressure, but after certain value of time, pressure reduces with time. It is also revealed that increase in α decreases with the pressure while behavior is reverse after certain value of time. Figure-3 depicts Δp vs. time t, for various values of β =1/5, 2/5, 3/5, 4/5 at $\overline{Q}$ =0.1, $\phi = 0.5$, $\lambda_1 = 1$, $\mathrm{Re} = 0.01$, $Fr = 0.01$, $A = \pi/3$, $\alpha = 1/5$. It is similar to figure-1, but the effect of β on pressure is opposite to that of α. The influences of relaxation time λ_1 =0.4, 0.6, 0.8, 1.0 and amplitude ϕ =0.4, 0.5, 0.6, 0.7 on the pressure–time curve are shown in figure-4 and figure-5 keeping other parameters fixed i.e. α =1/5, β =4/5, $\overline{Q}$ =0.1, $\mathrm{Re} = 0.01$, $Fr = 0.01$, $A = \pi/3$

It is found that, the effect of λ_1 is similar to α, but the pressure increases with increase in ϕ.

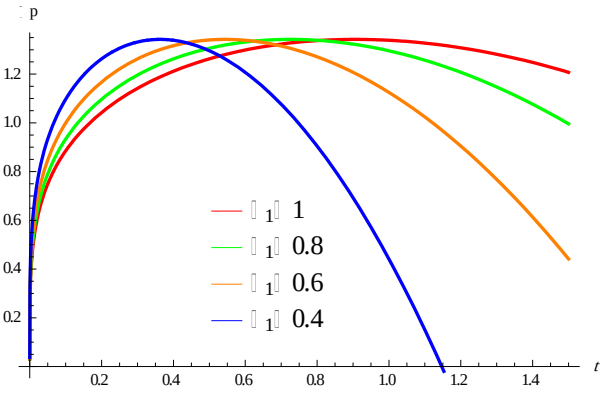

Figure 4- Pressure vs. time at $\overline{Q}$ =0.1, $\phi = 0.5, \beta = 4/5$, $\alpha = 1/5$, $\mathrm{Re} = 0.01$, $Fr = 0.01$, $A = \pi/3$

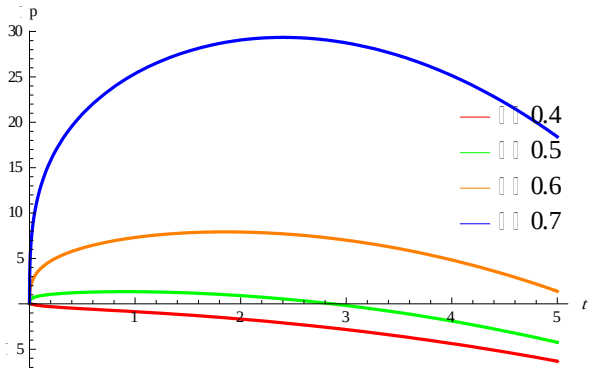

Figure 5- Pressure vs. time at $\overline{Q}$ =0.1, $\beta = 4/5$, $\lambda_1 = 1$, $\mathrm{Re} = 0.01$, $Fr = 0.01$, $A = \pi/3$, $\alpha = 1/5$

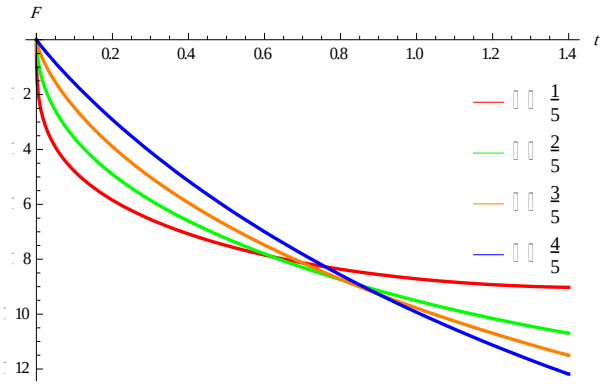

Figure 6- Friction force vs. time at $\overline{Q}$ =0.01, $\phi = 0.5, \beta = 4/5$, $\lambda_1 = 1$, $\mathrm{Re} = 0.01$, $Fr = 0.01$, $A = \pi/3$

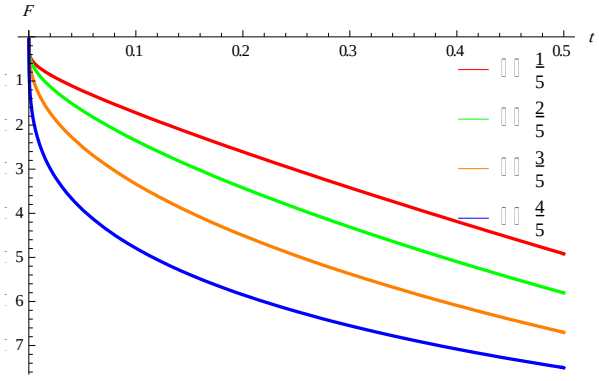

Figure 7- Friction force vs. time at $\overline{Q}$ =0.01, $\lambda_1 = 1$, $\mathrm{Re} = 0.01$, $Fr = 0.01$, $A = \pi/3$, $\alpha = 1/5$ $\phi = 0.5$.

Figure-6 and figure-7 describe the results obtained for the friction force F vs. the time t at various values of fractional parameters α, β. While figure-8 and figure-9 depict the variation of friction force F vs. the

time t at various values λ_1, ϕ Furthermore, the effects of important parameters such as α, β, λ_1 and ϕ on the friction force have been investigated. It is observed from figure-6 to figure-9 that, friction force has opposite behavior compared with pressure.

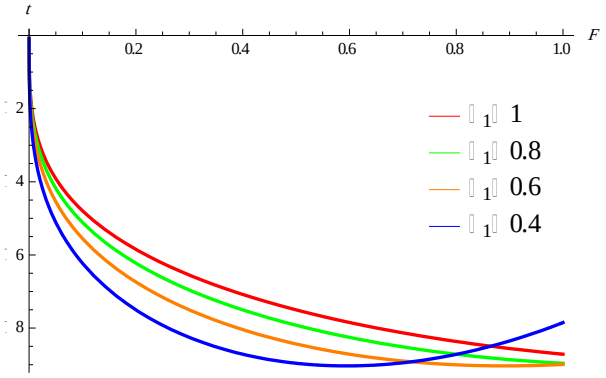

Figure 8- Friction force vs. time at $\phi = 0.5, \beta = 4/5,\ \alpha = 1/5$, Re = 0.01, $Fr = 0.01$, $A = \pi/3$, $\overline{Q}$ =0.01.

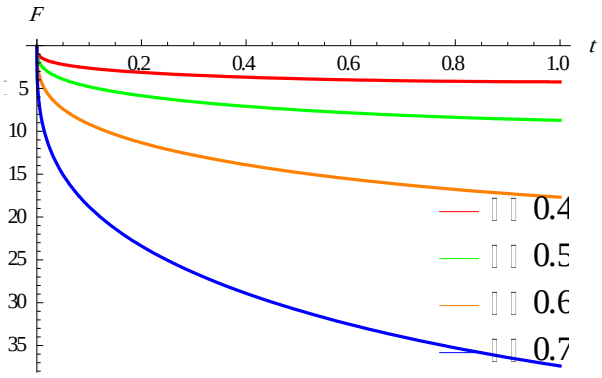

Figure 9- Friction force vs. time at $\overline{Q}$ =0.01, $\beta = 4/5$, $\lambda_1 = 1$, Re = 0.01, $Fr = 0.01$, $A = \pi/3$, $\alpha = 1/5$.

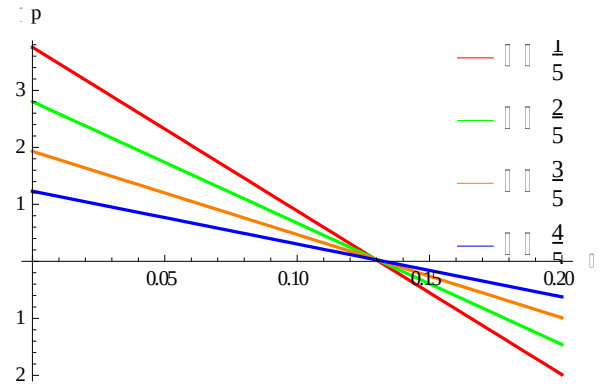

Figure 10- Pressure vs. averaged flow rate at t = 0.1, $\lambda_1 = 1$, Re = 0.01, $Fr = 0.01$, $A = \pi/3$, $\beta = 4/5$, $\phi = 0.5$

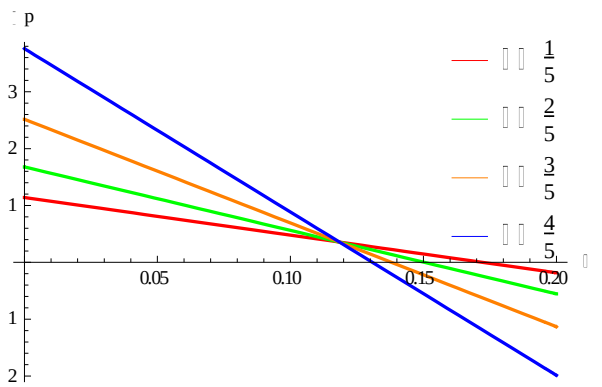

Figure 11- Pressure vs. averaged flow rate at t= 0.1, $\lambda_1 = 1$, Re = 0.01, $Fr = 0.01$, $A = \pi/3$, $\alpha = 1/5$ $\phi = 0.5$

Figure-10 and figure-11 depict the variation of Δp with averaged flow rate $\overline{Q}$ for different values of α, β and other parameters $\phi = 0.5, \lambda_1 = 1$, Re = 0.01, $Fr = 0.01$, $A = \pi/3$. It is observed that there is a linear relation between pressure and averaged flow rate, also an increase in the flow rate reduces the pressure. From the figures, it is also evident that the pressure decreases with increase in α while it increases with β. The variation of Δp with the averaged flow rate $\overline{Q}$ for different values of λ_1 at t = 0.1, $\beta = 4/5$, α = 1/5, β =4/5, Re=0.01, Fr=0.01 and A= $\pi/3$ is shown in figure-12. It is shown that the pressure diminishes as the relaxation time λ_1 increases. Figure-13 depicts the variation of Δp with the averaged flow rate $\overline{Q}$ for different values of ϕ at λ_1 =1.0, t =0.1, α = 1/5, β =4/5, =0.01, Fr=0.01 and A= $\pi/3$. It reveals that the pressure increases with increase in ϕ. The effect of Reynolds number (Re),

Froude number (Fr) on the pressure-averaged flow rate curve keeping other parameters fixed $t = 0.1,\ \phi = 0.5,\ \beta = 4/5,\ \lambda_1 = 1,\ A = \pi/3$ are depicted from figure-14 and figure-15. It is evident that the pressure increases with increasing the magnitude of Reynolds number while it decreases with increasing

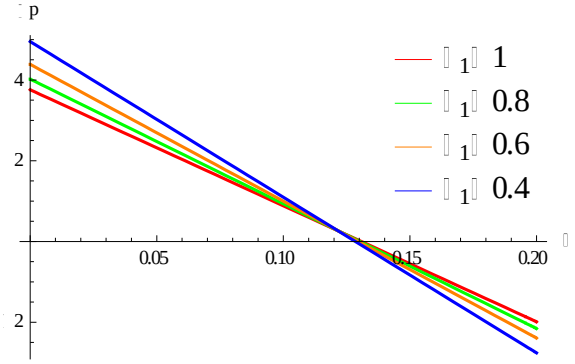

Figure 12- Pressure vs. averaged flow rate at t = 0.1, $\alpha = 1/5,\ \mathrm{Re} = 0.01,\ Fr = 0.01,\ A = \pi/3$ $\phi = 0.5,\ \beta = 4/5.$

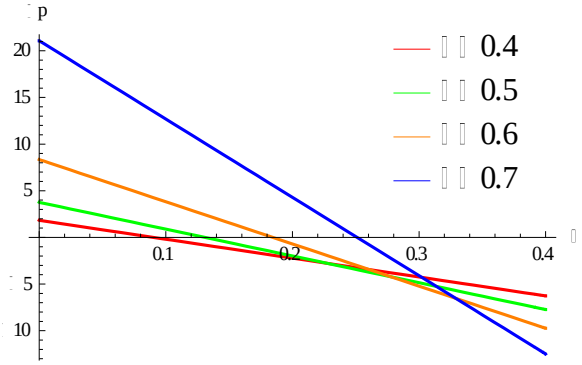

Figure 13- Pressure vs. averaged flow rate at t =0.1, $\beta = 4/5,\ \mathrm{Re} = 0.01,\ Fr = 0.01,\ A = \pi/3,\ \alpha = 1/5$ $\phi = 0.5,$

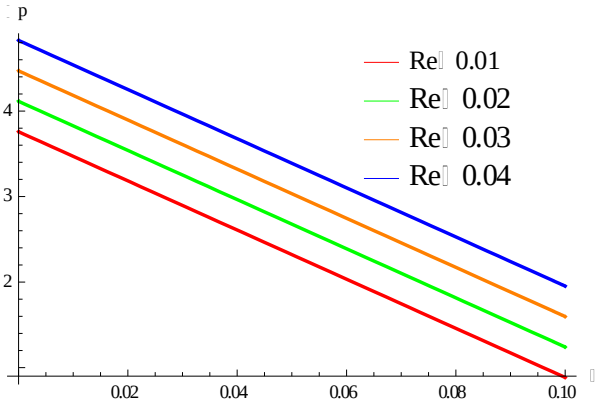

Figure 14- Pressure vs. averaged flow rate at t = 0.1, $\alpha = 1/5,\ Fr = 0.01,\ A = \pi/3,\ \phi = 0.5,\ \beta = 4/5.$ $\lambda_1 = 1$

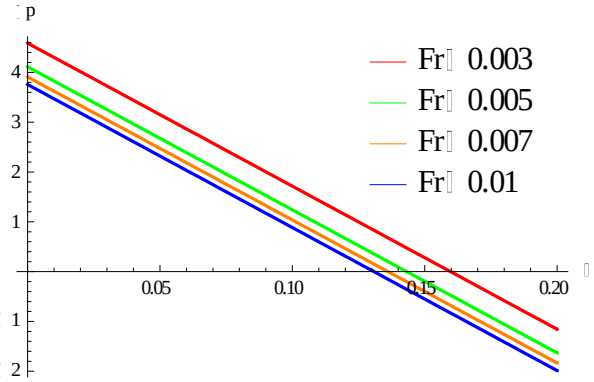

Figure 15- Pressure vs. averaged flow rate at t =0.1 $\beta = 4/5,\ \mathrm{Re} = 0.01,\ \lambda_1 = 1,\ A = \pi/3,\ \alpha = 1/5.\ \phi = 0.5,$

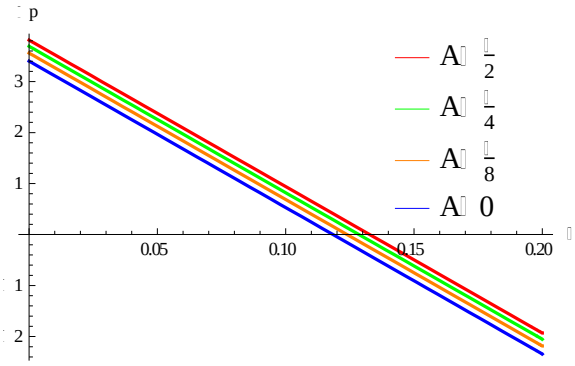

Figure 16- Pressure vs. averaged flow rate at t = 0.1, $\alpha = 1/5,\ Fr = 0.01,\ \mathrm{Re} = 0.01\ \ \phi = 0.5,\ \beta = 4/5,\ \lambda_1 = 1$

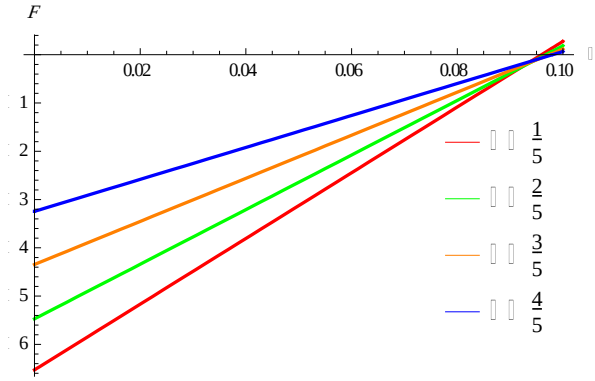

Figure 17- Friction force vs. averaged flow rate at t=0.1, $\beta = 4/5,\ \mathrm{Re} = 0.01,\ \lambda_1 = 1,\ A = \pi/3,\ Fr = 0.01,\ \phi = 0.5,$

The magnitude of Froude number in all regions. Figure-16, depicts Δp vs. $\overline{Q}$ for various values of inclination angle A= $\pi/2,\ \pi/4,\ \pi/8,\ 0$ at $t=0.1,\ \phi=0.5,\ \beta=4/5,\ \lambda_1=1,$ Re=0.01, and Fr = 0.01, it is found that the pressure increases in interval $0 \le A \le \pi/2$.

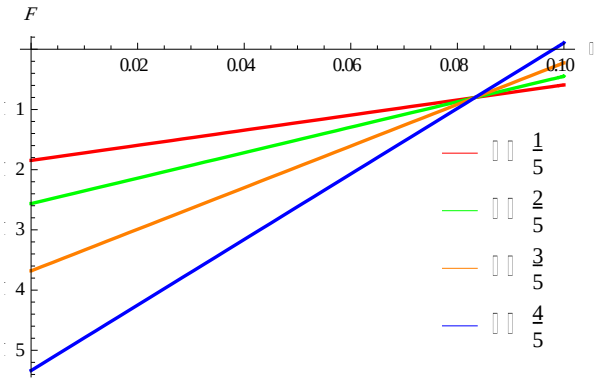

Figure 18- Friction force vs. averaged flow rate at, $\alpha=1/5,\ Fr=0.01,\ \mathrm{Re}=0.01\ \ \phi=0.5,\ \mathrm{A}\ \pi/3,$ $\beta=4/5,\ \lambda_1=1$, t = 0.1

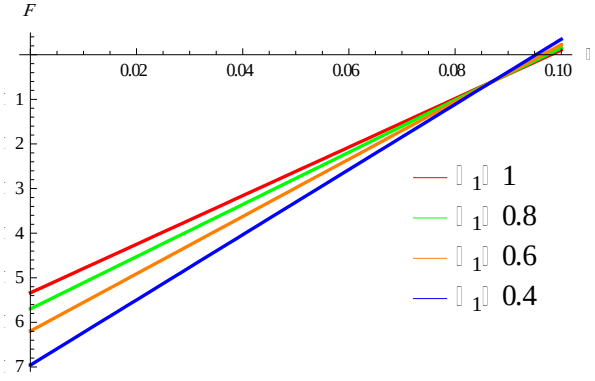

Figure 19- Friction force vs. averaged flow rate at t =0.1, $\beta=4/5,\ \mathrm{Re}=0.01,\ \alpha=1/5,\ A=\pi/3,\ Fe=0.01\cdot$ $\phi=0.5$

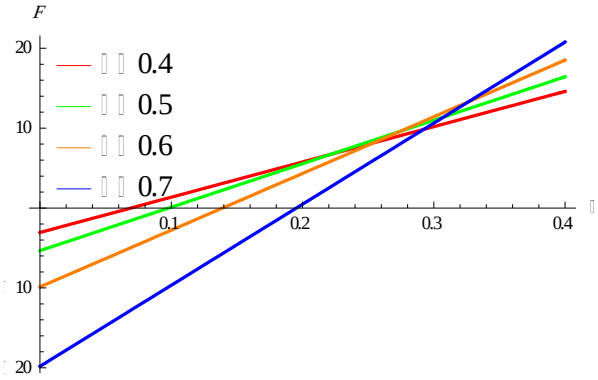

Figure 20- Friction force vs. averaged flow rate at $\alpha=1/5,\ Fr=0.01,\ \mathrm{Re}=0.01\ \ \beta=4/5,$ A= $\pi/3,\ \lambda_1=1,$ t = 0.1

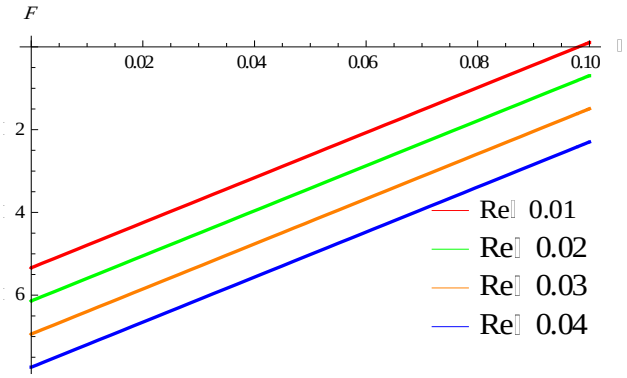

Figure 21- Friction force vs. averaged flow rate at t =0.1, $\beta=4/5,\ \lambda_1=1,\ \alpha=1/5,\ A=\pi/3,\ Fe=0.01,$ $\phi=0.5$

The streamlines on the center line in the wave frame of reference are found to split in order to enclose a bolus of fluid particles circulating along closed streamlines under certain conditions. This phenomenon is referred to as trapping, which is a characteristic of pumping motion. Since this bolus appear to be trapped by the wave, the bolus moves with the same speed as that of the wave. Figure-24(a-c) are drawn for streamlines for different values of the amplitude ratio (ϕ = 0.4 – 0.8) at $\overline{Q}=0.8$. Figures reveals that the size of trapped bolus increases when the magnitude of ϕ increases. Also figure-25(a-c) are drawn for streamlines for different values of the averaged flow rate ($\overline{Q}$ = 0.3 – 0.7) at $\phi=0.8$, it shows that the size of trapped bolus increases when the magnitude of $\overline{Q}$ increases. It is observed from Eq.(16) that the stream function is independent of ($\alpha,\ \beta, \lambda_1$, Re, Fr and A). This indicates the size of trapped bolus is unaltered with these parameters.

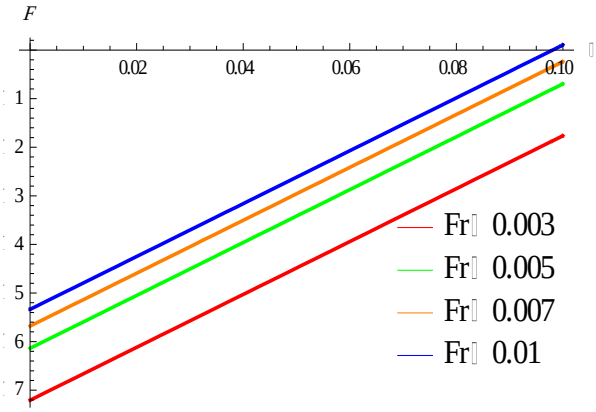

Figure 22- Friction force vs. averaged flow rate at $\alpha = 1/5,\ \phi = 0.5,\ \mathrm{Re} = 0.01\ \ \beta = 4/5,$ A= $\pi/3,\ \lambda_1 = 1,$ t = 0.1

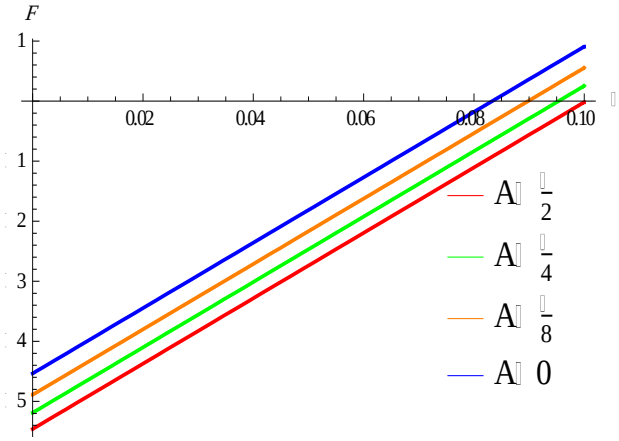

Figure 23- Friction force vs. averaged flow rate at t =0.1, $\beta = 4/5,\ \lambda_1 = 1,\ \alpha = 1/5,\ A = \pi/3,\ Fe = 0.01,$ $\phi = 0.5$

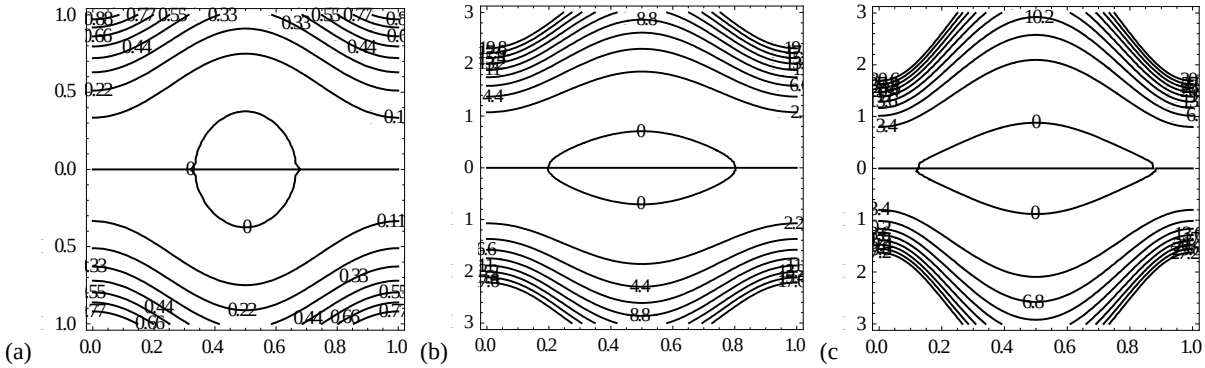

Figure 24- Streamlines in the wave frame at $\overline{Q} = 0.5$ for (a) $\phi = 0.4$, (b) $\phi = 0.6$, and (c) $\phi = 0.8$.

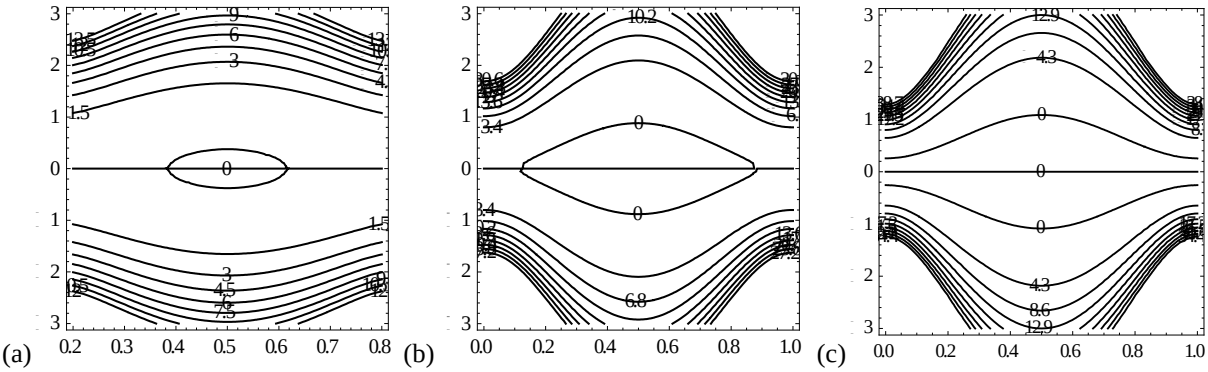

Figure 25- Streamlines in the wave frame at $\phi = 0.8$ for (a) $\overline{Q} = 0.3$, (b) $\overline{Q} = 0.5$, and (c) $\overline{Q} = 0.7$

5. Conclusions

The effects of fractional parameters and viscoelastic behaviors on peristaltic transport under the assumption of long wave boundary layer type approximation and low Reynolds number are discussed. ADM is used to find the approximate analytical solution. Main conclusions of the presented study are summarized as follows:

- Pressure increases with the increase in time; after a certain value of time, patterns become opposite.
- Averaged flow rate diminishes with increase in pressure.
- Pressure decreases with increase in α , but increases with increase in β .
- The behavior of relaxation time λ_1 on the pressure is similar to that of α .
- An increase in ϕ increases the pressure and the maximum averaged flow rate also increases with increase in ϕ .
- Pressure increases with increasing the magnitude of Reynolds number while it decreases with increasing the magnitude of Froude number, also increases with increasing of inclination angle.
- The variations of friction force with time and averaged flow rate show opposite behavior to that of pressure.
- The trapping increases with increasing the amplitude ratio or the average flow rate, while, it is unaltered with other parameters.

References

1. Elshehawey, E.F., Eldabe, N.T, Elghazy, E.M. 0 and Ebaid, A**. 2006**. Peristaltic transport in an asymmetric channel through a porous medium, *Appl. Math. Computer*. 182,pp: 140-150.
2. Burns, J.C. and Parkes, T. **1967**. Peristaltic motion. *J. Fluid Mech*, 29,pp: 731-743.
3. Barton, C. and Raynor, S. **1968**. Peristaltic flow in tubes. *Bull. Math. Biophys*, 30,pp: 663-680.
4. Fung, Y.C. and Yih, C.S. **1968**. Peristaltic transport. *J. Appl. Mech*, 35, pp: 669.
5. Shapiro, A.H., Jafferin, M.Y. and Weinberg, S.L .**1969** Peristaltic pumping with long wavelengths at low Reynolds number. *J. Fluid Mech*, 37, pp: 799-825.
6. Bohme, G. and Friedrich, R. **1983**. Peristaltic flow of viscoelastic liquids. *J. Fluid. Mech*, 128, pp:109–122.
7. Tsiklauri, D. and Beresnev, I. **2001**. Non-Newtonian effects in the peristaltic flow of a Maxwell fluid. *Phys. Rev. E* 64, 036303.
8. El-Shehawy, E.F., El-Dabe, N.T. and El-Desoki, I.M. **2006**. Slip effects on the peristaltic flow of a non-Newtonian Maxwellian fluid Mech. *Acta Mechanica*, 186, pp: 141–159.
9. Hayat, T. and Ali, N., Asghar, S. **2007**. Hall effects on the peristaltic flow of a Maxwell fluid in a porous medium. *Phys. Lett. A*, 363, pp: 397–403.
10. Hayat, T., Alvi, N. and Ali, N. **2008.** Peristaltic mechanism of a Maxwell fluid in an asymmetric channel, Nonlinear Analysis. *Real World Appl*, 9, pp: 1474–1490.
11. Ali, N., Hayat, T. and Asghar, S. **2009.** Peristaltic flow of a Maxwell fluid in a channel with compliant walls, *Chaos*, *Soliton. Fract*. 39, pp:407–416.
12. Hayat, T. and Ali, N .**2008.** Peristaltic motion of a Jeffrey fluid under the effect of a magnetic field in a tube. *Commun. Nonlinear Sci. Numerical Simulation*, 13, pp: 1343–1352.
13. Hayat, T., Ali, N., Asghar, S. and Siddiqui, A.M. **2006.** Exact peristaltic flow in tubes with an endoscope. *Appl. Math. Comput*er. 182, pp: 359–368.
14. Hayat, T., Ahmad, N. and Ali, N. **2008**. Effects of endoscope and magnetic field on the peristalsis involving Jeffrey fluid. *Commun. Nonlinear Sci. Numerical Simulation*, 13, pp: 1581–1591.
15. Hayat, T., Ali, N. and Asghar, S. **2007**. An analysis of peristaltic transport for flow of a Jeffrey fluid. *Acta Mech*, 193, pp: 101–112.
16. Tripathi, D., Pandey, S.K. and Das, S. **2010**. Peristaltic flow of viscoelastic fluid with fractional Maxwell model through a channel. *Appl. Math. Computer*. 215, pp: 3645–3654.
17. Tripathi, D**. 2011**. Peristaltic transport of a viscoelastic fluid in a channel, *Acta Astronaut*. 68, pp:1379-1385.
18. Tripathi, D. **2011**. Peristaltic flow of a fractional second grade fluid through a cylindrical tube. *Therm. Sci*. 15, pp: 167-173.
19. Tripathi, D. **2011**. Numerical and analytical simulation of peristaltic flows of generalized Oldroyd-B fluids. *Int. J. Numer. Meth. Fluids*. 67, pp: 1932-1943.
20. Tripathi, D. **2011**. A mathematical model for peristaltic flow of chime movement in small intestine. *Math. Biophys* .233, pp: 90-97.